

Mapping of tide and tidal flow fields along a tidal channel with vessel-based observations

Chunyan Li and Jack Blanton

Skidaway Institute of Oceanography, Savannah, Georgia, USA

Changsheng Chen

School of Marine Science and Technology, University of Massachusetts-Dartmouth, New Bedford, Massachusetts, USA

Received 2 June 2003; revised 23 January 2004; accepted 9 February 2004; published 1 April 2004.

[1] We present the results of a study focused on the tidal regime of a shallow channel with a large intertidal area. Data from a vessel-towed acoustic Doppler current profiler (ADCP) were used to infer tidal constituents for both tidal elevation and tidal current along an upstream portion of the Okatee River, South Carolina. The tidal elevation is estimated from the depth recorded by the moving ADCP. This tidal elevation is then used to correct the vertical coordinates of each depth bin below the ADCP for the velocity profiles. The ability to resolve both tidal elevation and velocity allows us to determine that the tide is a standing wave. A statistical analysis demonstrates that the along-channel velocity has a stronger tidal signal (larger R^2 values) than the across-channel velocity. When only the M_2 and mean components are included in the harmonic analysis, about 75% of the covered area along the ship track has a “good fit,” where at least 70% of the variability can be explained by the tidal and mean components. By adding the M_4 component to the harmonic analysis, an additional 2% of the covered area has “good fit” for the elevation, depth-averaged velocity, and mid-depth velocity, but 12% for the near-surface velocity. The observed spatial distribution of the residual flow is in reasonable agreement with that predicted by an unstructured grid, finite-volume coastal ocean model (FVCOM). *INDEX*

TERMS: 4594 Oceanography: Physical: Instruments and techniques; 4560 Oceanography: Physical: Surface waves and tides (1255); 4512 Oceanography: Physical: Currents; 4235 Oceanography: General: Estuarine processes; *KEYWORDS:* harmonic-statistic analysis, ADCP surveys, tidal creek

Citation: Li, C., J. Blanton, and C. Chen (2004), Mapping of tide and tidal flow fields along a tidal channel with vessel-based observations, *J. Geophys. Res.*, 109, C04002, doi:10.1029/2003JC001992.

1. Introduction

[2] Vessel-based acoustic Doppler current profilers (ADCPs) have long been used to measure velocity profiles in many applications [e.g., *Lwiza et al.*, 1991; *Brubaker and Simpson*, 1999]. A vessel-based ADCP records vertical profiles of velocity vectors from the surface along a series of vertical bins. The ADCP is mounted either on a towed sled or on one side of a moving vessel with its transducers placed just below the surface and facing downward. Discrete velocity data are measured in a series of vertical “bins.” The first data point (or the first valid bin) is away from the transducer by a distance determined by the user-defined vertical bin size, the speed of sound, and the “blank after transmit” (a distance required by the instrument design for echo data processing and data quality). The axes of the transducers are designed to have a 20° – 30° angle from the axis of the instrument to resolve the three-dimensional velocity vector. This design causes “sidelobe” interference (invalid velocity) near the bottom within a thin layer of the

water column. Excluding these thin surface and bottom layers, the vertical profiles of the velocity can be used. Each bin along the vertical axis is referenced from the surface which is defined with a given vertical coordinate (e.g., $z = 0$). In reality, the water surface is moving due to waves and tides, particularly in coastal water where tidal forcing is significant. This can cause a change of the vertical coordinate of each bin (unless the surface change is smaller than the ADCP bin size and much smaller than the mean water depth). Previous studies have treated the vertical coordinate of each bin as a constant for convenience. Although ADCP transducers can measure water depth, this has not been used in correcting the effect of variable surface elevation due to tidal oscillation. In shallow waters where water depth can be as shallow as $O(10)$ m and tidal range on the order of $O(1)$ m, this can be problematic. This problem can be even more remarkable in tidal creeks (typically 3–10 m deep) with large tidal range, for example, ~ 3 m as in South Carolina and Georgia.

[3] *Li et al.* [2000] demonstrated that using the water depth measured by the ADCP transducers, tidal elevation can be estimated if there are enough observations along a pre-defined route. The quality of the estimation depends

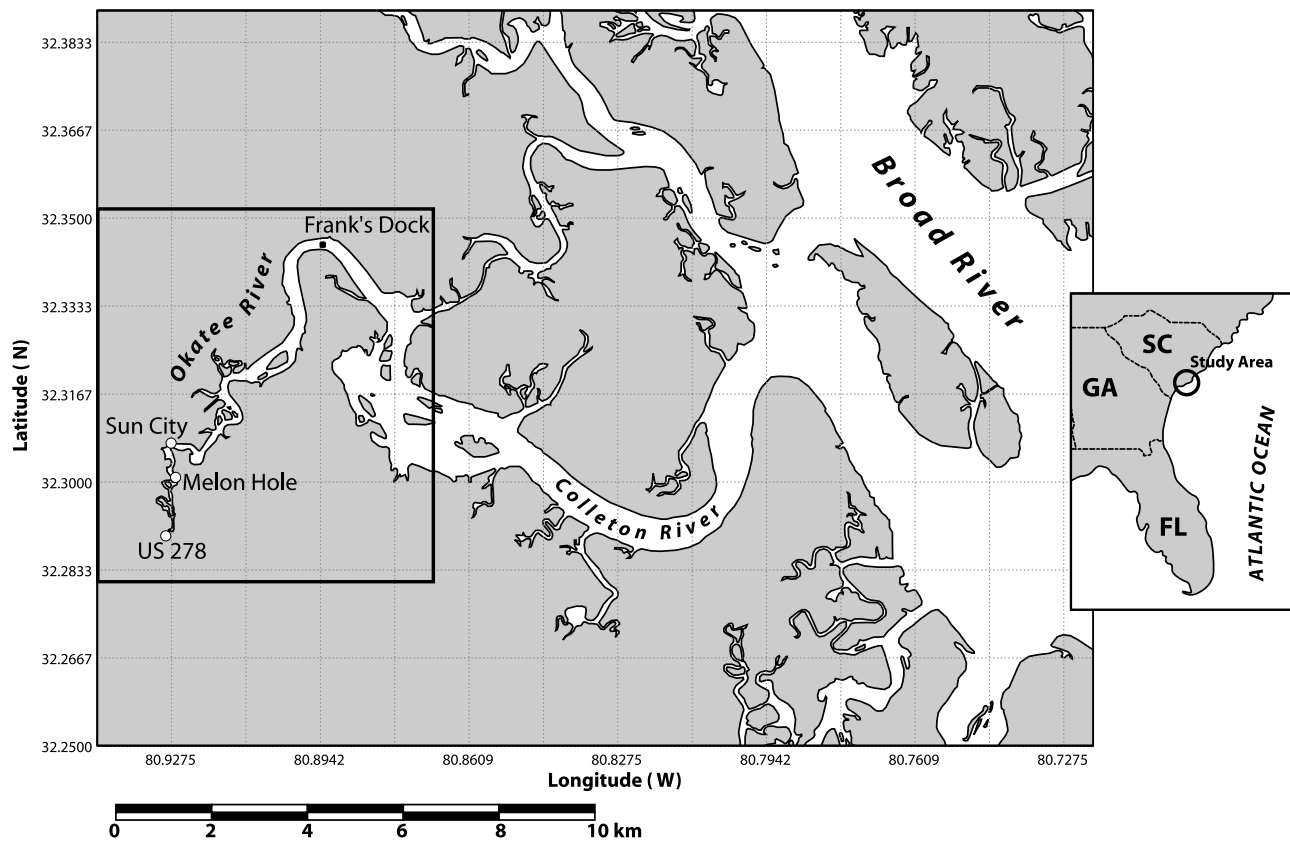


Figure 1. Study area: Okatee River/Creek, South Carolina.

upon several factors, which include (1) GPS error, (2) slope of the water bottom, (3) speed of the vessel, and, of course (4) the accuracy of the transducers. GPS error can be roughly considered to be a nonvariable for a specific instrument (strictly speaking, the error can be a function of time, but it should be within certain limits specified by the manufacturer). Intuitively, as long as the GPS error is not larger than the spatial resolution, which is roughly the product of the mean vessel speed and the averaging interval, we can reasonably ignore it. The error of the depth measured by the transducers of our ADCP is on the order of 1% of the total water depth. If this error is much smaller than the tidal range, we can also ignore it. For instance, in 10 m of water with a 2-m tidal range, the error of the depth measurement is 1% of 10 m, which is 10 cm, a value that is much smaller than the 2-m tidal range. The most variable error is caused by the bottom slope. The larger the slope, the larger the possible error. Observations [Li *et al.*, 2000] at the mouth of the Chesapeake Bay ($\sim 3\text{--}28$ m) showed that with an average vessel speed of about 5 knots (2.5 m/s), 70% of the depth variability obtained from observations within the same segment of 80 m along the ship track can be explained by tidal oscillation if the bottom slope is $O(0.003)$ or less. The optimal size of the cell for data analysis was found to be the same as the spatial resolution of the observations, i.e., the product of the mean vessel speed and the averaging interval (30 s in the study of Li *et al.* [2000]), which yielded a spatial resolution of about 75 m at 5-knot vessel speed.

[4] In this study, we apply the method of Li *et al.* [2000] to the Okatee River of South Carolina to obtain both tidal

elevation and tidal velocity along the main channel within a 10-km distance. By this method, we will be able to determine the spatial distribution of the phase difference between tidal elevation and tidal velocity from a vessel-towed ADCP and to determine the tidal characteristics (e.g., whether the tide is a progressive or standing wave). We will use a harmonic-statistical analysis [Li *et al.*, 2000] to infer the tidal constituents of both elevation and velocity and various statistics of the observations.

2. Study Area and Objective of Study

[5] Located in the South Atlantic Bight 35 km northeast of Savannah, Georgia, the Okatee River is part of a larger tidal creek system that empties into the Broad River, then into Port Royal Sound, and finally into the ocean 30 km to the southeast of the Okatee's headwaters (Figure 1). This study focuses on the upstream portion of the Okatee River within a 10-km distance from its headwaters with the water depth between 0 and 8 m. The channel meanders and has two nearly 180° bends. The channel width is on the order of 200–300 m. The river is surrounded by extensive intertidal salt marsh. The upstream 1 km of the study area is often exposed at low tide. Tidal range during spring tide can be as much as 3 m or more, while the neap tide tidal range is about 1.5 m and the mean tidal range is about 2.5 m. Velocity field has large spatial differences with the maximum amplitude varying between 0.8 and 1.1 m/s from neap to spring. There is very little freshwater discharge into the system. Because of the shallow water depth and strong tidal

forcing, the water column is well mixed. Dominant factors that affect the flow field are the tide, channel meanders, and the surrounding intertidal salt marsh that may store water mass particularly at high tides.

[6] Okatee River is the study site of the Land Use-Coastal Ecosystem Study (LU-CES), a 4-year project funded by the NOAA Coastal Ocean Program (<http://www.lu-ces.org>). The principal goal of LU-CES is to develop scientifically based models that can be used by natural resource agencies and policy makers to identify and develop minimal impact scenarios for development within the coastal plain of South Carolina and Georgia. The research mainly focuses on physical and biological processes in critical tidal creek ecosystems in the region's sensitive and unique salt marsh estuaries. As a physical component of the LU-CES project, one of the objectives of this study is to validate a fine-scale finite volume numerical model [Chen *et al.*, 2003] applied to this region. This study contributes to this objective by obtaining high-resolution data on the velocity distribution along the main channel and determining the tidal constituents for surface elevation and tidal velocity. We will focus on the techniques of data analysis, results from the analysis, and some general comparison between data and model results, as the validation of the model will be presented in a separate paper (C. Chen *et al.*, manuscript in preparation, 2004).

3. Observations

[7] Observations were made on March 8, 2001, using a 7-m-long fiberglass vessel from the Skidaway Institute of Oceanography (SkIO), the twin engine catamaran R/V *Gannet*. The date of the observations was 1 day before the full moon, and the tide was at the spring tide. There was no major wind event during the observations. An RDI 600-KHz Broadband ADCP with bottom tracking was mounted looking downward on a metal sled and towed on the starboard side of the boat. A Furuno-36 Differential Global Positioning System (GPS) receiver was used for the navigation and recording of the time and position. The standard error of this GPS has been determined to be $O(10)$ m with a test at a fixed location at SkIO after the observations. The ADCP was configured to sample 0.5-m vertical bins, and the data were averaged at 15-s intervals. A predefined route with a total length of about 8 km was followed by the boat repeatedly 15 times over a 13-hour period. A Sea Bird Electronic, Inc., surface thermosalinograph (SBE-21) was used to record the water temperature and salinity continuously through a water pump system equipped with the R/V *Gannet*. An SBE-25 CTD was also used for recording profiles of water temperature and salinity. The boat speed was maintained at about 6 knots (3 m/s) throughout the observations except during CTD casts and for a short time during a change of crew in the middle of the survey. The CTD data, however, showed no stratification along the entire route during the survey. The observations recorded a surface water temperature between 13° and 15°C . Salinity during the survey changed between 32.2 and 33.8 PSU. As a result, the density ranged between 1024.0 and 1025.3 kg/m^3 . These observations show that

during the period of observations, the Okatee River was well mixed with negligibly small along channel density gradients.

4. Analysis and Results

4.1. Grid System for Data Analysis

[8] Because of the strong and changing current from flood to ebb, as expected, the vessel could not exactly follow the same track. The error from the differential GPS itself also makes the track variable (error ~ 10 m). To analyze the data from the moving vessel (including those from the ADCP and the surface sensors for water temperature and salinity), we mask a rectangular grid onto the study area and choose a 50 m by 50 m cell size to group the data. All data points falling into a given cell will be treated as if from a single point defined by the center position of the cell. We then order all the data from within a given cell according to their time to form a time series for harmonic and statistical analyses. In a complete tidal cycle, any cells that have either no data or very little data (less than six points) are treated as empty cells, and the analyses are skipped. The size of the cell has a small effect on the statistical characteristics, but has no effect on the structure of the flow [Li *et al.*, 2000]. If the cell size is too small, there are not enough data points within each cell because the vessel may pass through a cell within the time interval of data average during a particular repetition. If the cell is too large, there may be too much scattering of the data points because of the inherent spatial variability of the flow field as a function of the position and local depth. In our survey, the averaging interval is 15 s, the vessel speed is about 3 m/s, and the horizontal resolution is about 45 m, a value roughly the same as our cell size.

4.2. Correction of Vertical Coordinate for Velocity Data

[9] To correct the vertical coordinate of each bin for the velocity profile at a given time, we first use the water depth obtained from the ADCP at the center of each cell to form a time series. We then apply a harmonic analysis to this time series for each cell to obtain (1) the average water depth (h_0) along with (2) the amplitude (a) and phase (θ) of the surface elevation at each cell. The surface elevation is then expressed as $\zeta = a \sin(\omega t + \theta)$, in which ζ , ω , and t are surface elevation, M_2 tidal frequency, and time, respectively. Without a correction of the vertical coordinate, at any given time, the first bin of the velocity profile will be at a depth of A_1 , a value calculated by the RDI software based on the depth of the transducer, blanking distance, sound speed, and the vertical bin size. In our case, A_1 is 1.75 m. To correct the vertical coordinate, we have to consider the variation of the surface elevation. At time t , the first velocity bin has a vertical coordinate of $\zeta - A_1$. Similarly, at the N th bin, the vertical coordinate is $\zeta - A_1 - B \times (N - 1)$, where B is the bin size. We then redefine the vertical bins relative to the mean surface ($z = 0$) and interpolate the velocity profile at any time onto the new vertical bins.

4.3. Harmonic-Statistical Analysis

[10] After excluding empty cells and after all the ADCP data are ordered within each cell with vertically corrected

velocity profiles, we then apply the harmonic-statistical method [Li *et al.*, 2000] as briefly described below. We assume that a time-dependent variable denoted by v within a given cell can be expressed as

$$v = \alpha_0 + \sum_{j=1}^M [\alpha_j \cos(\omega_j t) + \beta_j \sin(\omega_j t)], \quad (1)$$

in which α_j and β_j are the harmonic constants, ω_j is the j th tidal frequency, t is time, M is the total number of tidal frequencies selected, and the subscript j represents integers between 0 and M . Equation (1) can also be expressed in a matrix format,

$$V = Ax, \quad (2)$$

in which V is the variable vector for all v values measured at different times in the given cell, A is a matrix, and x is a vector of harmonic constants to be determined, i.e.,

$$V = (v_1, v_2, \dots, v_N)^T \quad (3)$$

$$x = (\alpha_0, x_1, x_2, \dots, x_{2M})^T, \quad (4)$$

$$x_{2k-1} = \alpha_k, \quad x_{2k} = \beta_k, \quad k = 1, 2, \dots, M,$$

where T denotes the transpose of the vector, and the matrix A is defined by

$$A = \begin{pmatrix} 1 & a_{1,1} & a_{1,2} & \cdots & a_{1,2M} \\ 1 & a_{2,1} & a_{2,2} & \cdots & a_{2,2M} \\ \vdots & \vdots & \vdots & \vdots & \vdots \\ 1 & a_{N,1} & a_{N,2} & \cdots & a_{N,2M} \end{pmatrix}, \quad (5)$$

where N is the total number of observations and

$$a_{i,2k-1} = \cos(\omega_k t_i), \quad a_{i,2k} = \sin(\omega_k t_i), \quad (6)$$

$$i = 1, 2, \dots, N, \quad k = 1, 2, \dots, M.$$

When the number of observations (N) is much larger than the number of tidal frequencies (M), equation (2) is overdetermined and we can use a least squares method to estimate the harmonic constants (vector x). As a result, the best statistical estimate of x is

$$\hat{x} = (A^T A)^{-1} A^T V. \quad (7)$$

The error estimate or the residual sum of the squares is

$$R_{SS} = (V - A\hat{x})^T (V - A\hat{x}), \quad (8)$$

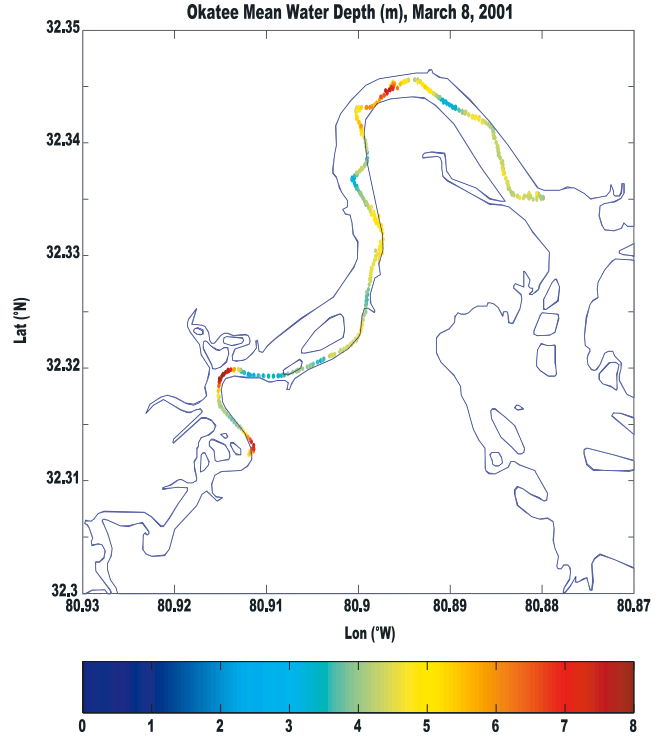


Figure 2. Color-coded plot for the mean water depth (m) calculated from the harmonic-statistical analysis of the depth data measured by the ADCP. Analysis is carried out for data grouped within each 50 m by 50 m cell.

and the standard deviation (or the standard error) of the fitting and the coefficient of determination are, respectively,

$$\hat{\sigma} = \sqrt{\frac{R_{SS}}{N - (2M + 1)}} \quad (9)$$

$$R^2 = 1 - \frac{R_{SS}}{R_{VV}}, \quad (10)$$

in which R_{VV} is

$$R_{VV} = \sum_{i=1}^N \left(v_i - \sum_{j=1}^N v_j / N \right)^2. \quad (11)$$

Equation (10) is the fraction of variability explained by the tidal constituents and the mean, which is 1 minus the unexplained variability R_{SS}/R_{VV} .

4.4. Application of Harmonic-Statistical Method

[11] The harmonic-statistical analysis is applied to both the water depth and the velocity profiles measured from the ADCP. The short time period of the survey (13 hours) allows us only to resolve the semidiurnal tides. Since this area is dominated by semidiurnal tides anyway, we will choose M_2 as one of the tidal frequencies in the harmonic-statistical analysis. Because of the short length of observations, we are unable to distinguish between the different

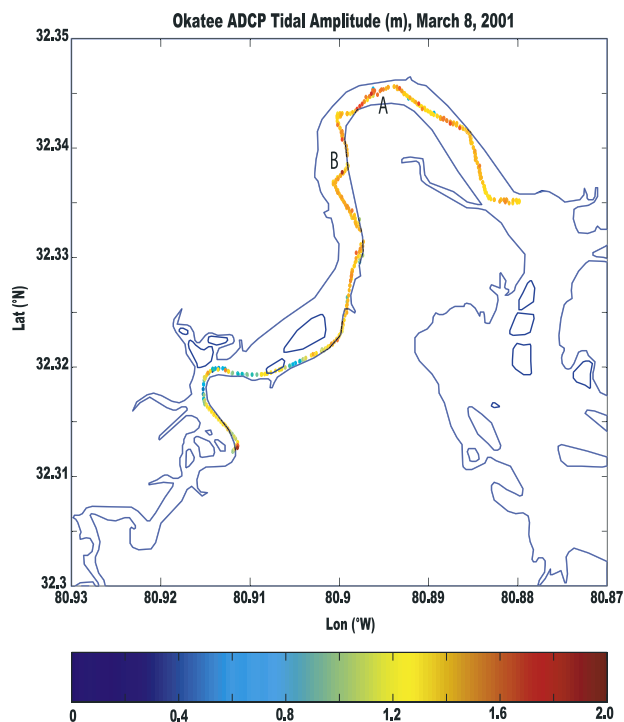


Figure 3. Color-coded plot for the M_2 tidal amplitude of surface elevation (m) within 50 m by 50 m cells.

semidiurnal tides (e.g., N_2 and M_2). Therefore the semidiurnal tide selected (M_2) will represent all semidiurnal tides [Proakis and Manolakis, 1992]. Furthermore, because of the limited number of observations (15 repetitions), we are restricted by the Nyquist frequency and will not be able to resolve higher frequency overtones and compound tides except for the M_4 [Proakis and Manolakis, 1992]. As a result, we only include the M_2 and the M_4 as the tidal frequencies of interest. Here M_4 is the double frequency of the M_2 tide and is generated by the nonlinear terms of advection, continuity, and bottom friction [Aubrey and Speer, 1985; Parker, 1991].

4.5. Tide

[12] Results show that the tidally averaged water depth is between 3 and 8 m with a spatial mean of about 5 m (Figure 2). The coastline is drawn using NOAA's data, which have errors at places, and the ship track is occasionally shown on land due to these errors. From Figure 2 we can see that the deepest water (~ 8 m) is at the three major turns of the channel. Most of the rest of the channel is below 5 m. The M_2 tidal amplitude has a relatively small variation along the channel (Figure 3) with an amplitude of about 1.4 m. Since the harmonic analysis yields both tidally averaged water depth and tidal amplitude, the standard error of the analysis can be considered as either that of the water depth or that of the tide. This standard error is mostly about 0.2 m in areas with relatively gradual variation of the bottom slope, but it increases to more than 1 m at a few places with large bottom slope or irregular spatial variations in depth where the R^2 values are much less than 1 (0.1–0.3). The average standard error for the tide is about 0.3 m. This error can be caused by wind effect and observational errors (such as those due to bottom slope and GPS errors).

The M_4/M_2 ratio of tidal amplitudes is about 0.18 with some variation (between 0.08 and 0.25) along the channel but with no clear pattern. The mean ratio between the M_4 and M_2 tidal amplitude (0.18) is higher than that from a pressure sensor on a bottom mounted upward-looking ADCP of a later deployment. This additional pressure sensor was deployed at bottom at the “Franks’ Dock” (Figure 1) between March 27 and April 25, 2001, and the calculated M_4/M_2 ratio is about 0.11. The lack of clear pattern in the M_4/M_2 ratio and the higher M_4/M_2 ratio from the towed ADCP are probably in part caused by the noisy nature of the water depth data from the moving ADCP along a highly variable bottom. This can be verified by calculating the mean M_4/M_2 ratio for “very good fit” only: for those data with R^2 values equal to or larger than 0.8, which yields 0.14, which compare more favorably to 0.11, the value from the bottom mounted pressure sensor. Note that on the basis of Li *et al.* [2000], and with some moderate modifications in the observational procedures, the data quality can be improved. These modifications may include (1) selecting a higher precision GPS unit, (2) avoiding crossing large changes in bottom slope at high speed, and (3) operating the research vessel at a slower and steady speed. By doing these, we expect that the estimate of tidal elevation can be more accurate.

4.6. Tidal Flow

[13] Tidal flow is mostly along the channel, dominated by M_2 constituent, and is slightly asymmetric [Blanton *et al.*,

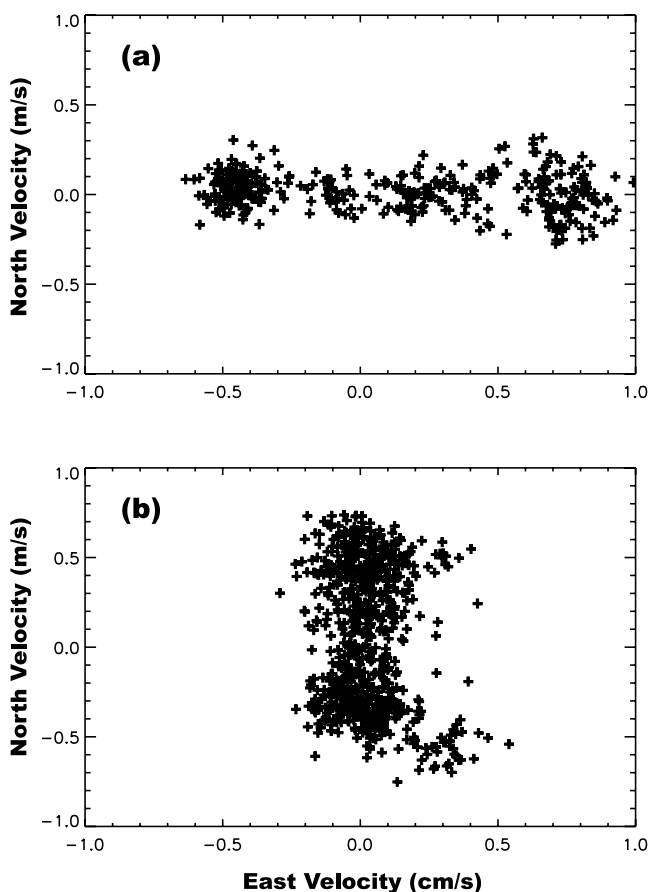


Figure 4. East velocity versus north velocity at (a) point A shown in Figure 3 and (b) at point B shown in Figure 3.

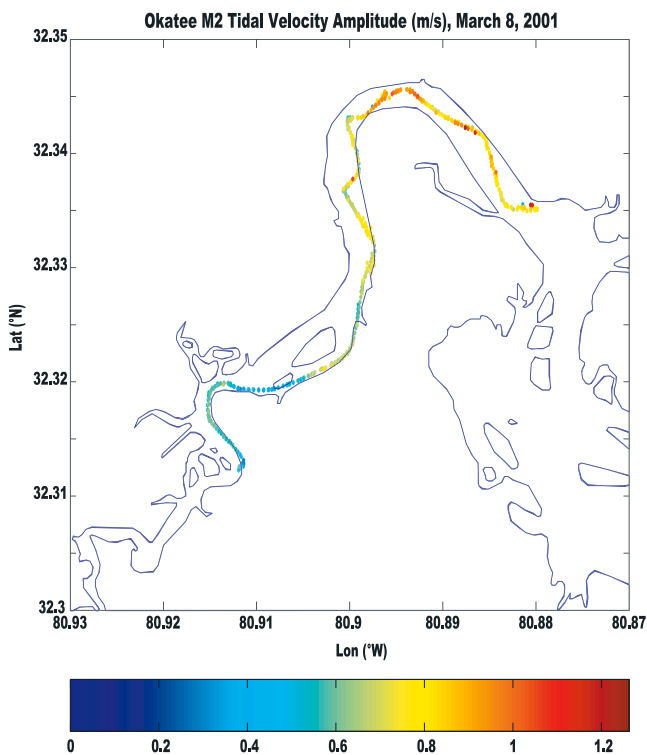


Figure 5. Color-coded plot for the amplitude of the M_2 velocity magnitude (m/s) within 50 m by 50 m cells at subsurface (2 m below the low water level).

2002] such that velocity at maximum ebb is slightly larger than that at maximum flood at most places. As an example, the surface east (north) velocity at point A shown on Figure 3 between -80.897°W and -80.894°W , where the channel is almost east-west oriented, ranges between -0.7 (-0.3) and 1.0 (0.3) m/s (Figure 4a) with a mean east (north) velocity of about 0.12 (0.01) m/s. Whereas the surface east (north) velocity at point B shown on Figure 3 between 32.33°N and 32.335°N , where the channel is almost north-south oriented, ranges between -0.25 (-0.7) and 0.4 (0.7) m/s (Figure 4b) with a mean north (east) velocity of about 0.05 (0.03) m/s.

[14] The vertical structure of the flow shows no strong shear, and the weak vertical shear of the horizontal velocity is apparently caused by friction, not stratification, because there is little freshwater discharge into the system (verified by the uniform salinity distribution). By correcting the vertical coordinates of each velocity bin relative to the ADCP along the water column, the velocity amplitude at different depths is determined. We have found as much as 15% difference for the tidal amplitude and mean flow between results with and without the depth correction. The near-surface velocity (at ~ 2 m below the surface) is slightly larger than that below and that of the depth-averaged values.

[15] The amplitude of the velocity magnitude ($\sqrt{u(r,t)^2 + v(r,t)^2}$) decreases significantly toward upstream. This is typically represented by the velocity at subsurface (2 m below the low water level, Figure 5). The small variability in the amplitude of the elevation and a relatively large change in velocity is a signature of a standing wave in

a short channel. This is because in a short channel, the amplitude of the reflected wave cannot be strongly reduced by the bottom friction such that the incident wave and the reflected wave superimpose together to form a standing wave. The short channel does not allow a significant spatial change of elevation, and at the same time, the no-flow boundary condition at the headwaters requires a rapid decrease of velocity to zero [Li, 1996, Figures 4.1 and 5.2; Li, 2001, Figure 6]. Indeed, the M_2 tidal elevation and depth-averaged along channel tidal velocity have an average phase difference of $88.9 \pm 9.5^\circ$ (Figure 6), indicating a standing wave condition. Without the ability to resolve the tidal elevation, it is not possible to calculate this phase difference and determine the characteristics of the tidal wave, unless an additional mooring instrument is used. The amplitude of M_2 along-channel tidal velocity ranges between 0.4 and 1.1 m/s. Velocity amplitude in shallower waters tends to be smaller, an effect attributed to bottom friction as shown by two-dimensional [Li and Valle-Levinson, 1999] and three-dimensional [Li, 2001] analytical models. Specifically, the velocity amplitude in waters of 3 to 4 m has a value of about 0.35 to 0.60 m/s, while in waters of 5 m to 6 m the velocity amplitude is about 0.7 to 0.9 m/s, respectively. The standard error of the velocity is between 0.05 and 0.20 m/s with the average value of about 0.12 m/s. The mean flow along the ship track shows dominant downstream flow and a clear signal of channel meandering; that is, the mean flow turns as the channel turns at most places (Figure 7).

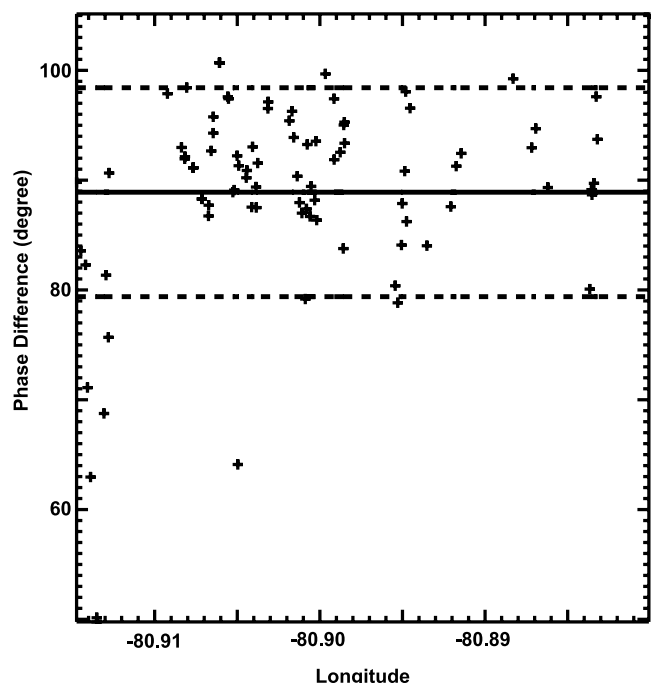


Figure 6. Phase difference (degree) between the M_2 tidal elevation and the M_2 velocity within 50 m by 50 m cells along the channel. For convenience, we have used longitude to roughly denote the location of the cell. In the calculation of the phase difference, we have limited only those data with R^2 values larger than 0.9. The solid and dashed lines indicate the mean and ± 1 standard deviation.

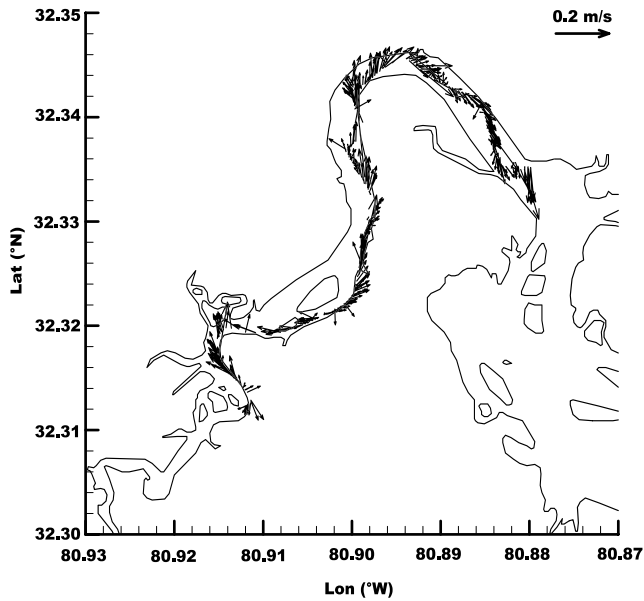


Figure 7. Mean velocity vector within 50 m by 50 m cells along the channel.

[16] The M_4/M_2 ratio of the velocity amplitudes yields a mean value of about 0.20. This value is consistent with the value (0.21) from the bottom-mounted ADCP deployed at the Frank's Dock (Figure 1) after the spatial survey (March

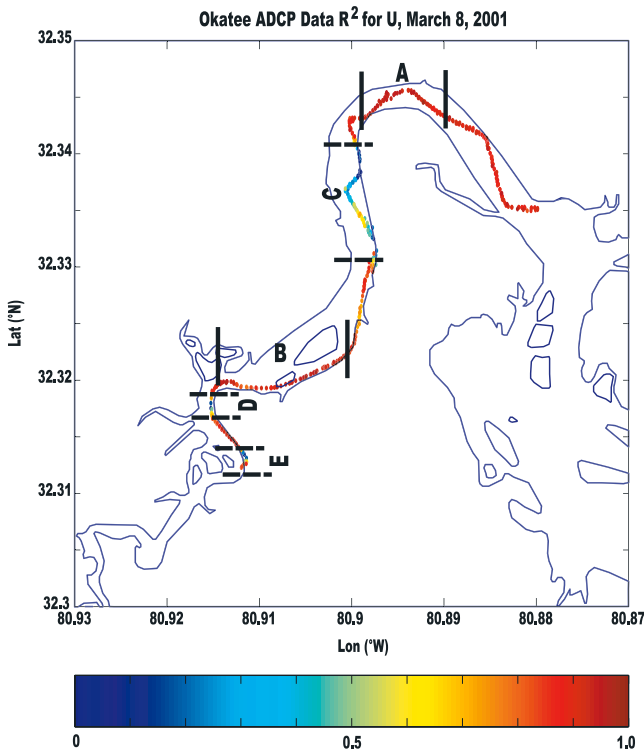


Figure 8. Color-coded plot of R^2 for east velocity component. The marked segments A and B, which are almost east-west oriented, between the solid line bars indicate the areas of close-to-unity R^2 values for the east velocity. The marked segments C, D, and E, which are almost north-south oriented, between the dashed line bars indicate the areas of much smaller R^2 values for the east velocity.

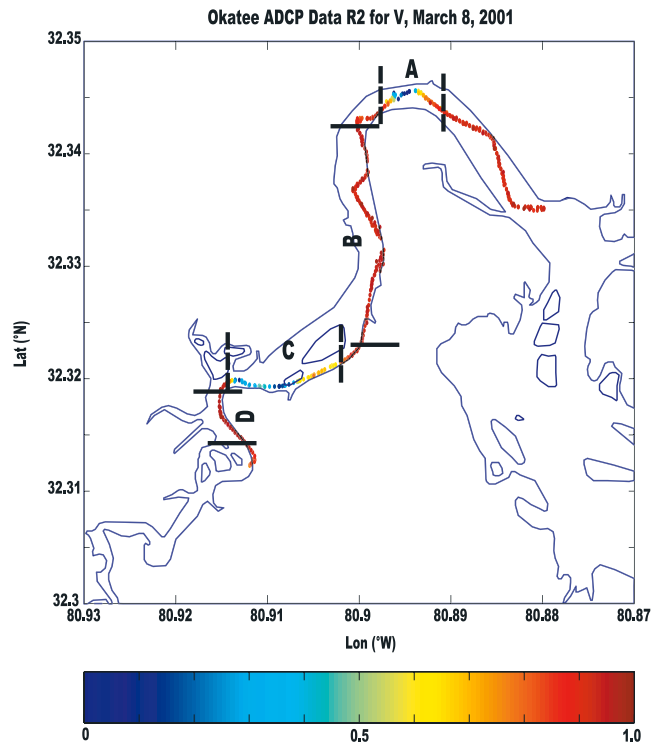


Figure 9. Color-coded plot of R^2 for north velocity component. The marked segments B and D, which are almost north-south oriented, between the solid line bars indicate the areas of close-to-unity R^2 values for the north velocity. The marked segments A and C, which are almost east-west oriented, between the dashed line bars indicate the areas of much smaller R^2 values for the north velocity.

27 to April 25, 2001). Note that the data from the bottom-mounted ADCP need no correction for the vertical coordinates. Again, the M_4 component of velocity is a result of nonlinearities in advection, continuity, and bottom friction [Parker, 1991] that is common for a shallow tidal creek. The phase of M_4 , however, was quite noisy, and there was no useful conclusion that we could reach. This is probably because the M_4 signal was too small and the moving vessel introduced a comparatively large error.

4.7. Variability in Along- and Cross-Channel Velocity Components

[17] The harmonic-statistical analysis also yielded interesting results that showed the differences in the variability between the along- and the cross-channel velocity components. Although only the east and north components of the velocity are analyzed, they may be good approximations for along- and across-channel velocity components at several segments of the channel where it is oriented roughly east-west or north-south as shown in Figures 8 and 9. Figures 8 and 9 are color-coded plots of the R^2 value for the east and north components of the depth-averaged velocity, respectively, within the 50 m by 50 m cells along the ship track. It is clear that at most positions, the R^2 value is close to 1, indicating that data within these cells behave mostly as tidal oscillations plus a mean value. There are, however, a few segments along which the R^2 value for the east or north velocity is low, indicating that a larger

percentage of the variation is not tidal. The tidal signal within these segments is weaker, and the variation of the velocity cannot be explained well by a tidal oscillation plus a mean flow. Notice that these low R^2 values are at places where the east (or north) velocity component contributes mostly to the cross-channel velocity, while the high R^2 values are at places where the east (north) velocity component contributes mostly to the along-channel velocity. This indicates that the along-channel velocity has a stronger tidal signal than the cross-channel velocity and the cross-channel velocity is considerably noisier. A possible explanation of this difference between the velocity components is that the main force balance is tidal and along the channel, and the tidal pressure gradient across the channel is relatively small such that to a larger extent (compared to the along-channel situation), it is subject to the effects of the irregular lateral boundaries and depth variations which produce nontidal flow components through nonlinear processes.

5. Discussion

5.1. Mean Flow

[18] The cause of the dominant downstream flow may be due to two effects. First, the boat cannot navigate in very shallow water (<2 m), which is covered by water during high tides but exposed during low tides. The shallow water is not accessible to evaluate the net transport outside of the main channel. It is likely that a compensating upstream flow exists. Second, the record from another pressure sensor moored near point A of Figure 3 from February 28 to April 26, 2001, shows that the mean water surface was dropping, during the times of the vessel-based observations, which is consistent with an overall downstream flux of water. Therefore, even if there is an upstream flow of water in the shallower areas including in and around the salt marsh, it probably cannot compete with the downstream flow of the main channel. As a result, the net transport may still be downstream. Unlike the downstream flux of water in rivers with significant freshwater discharge, the net downstream flow

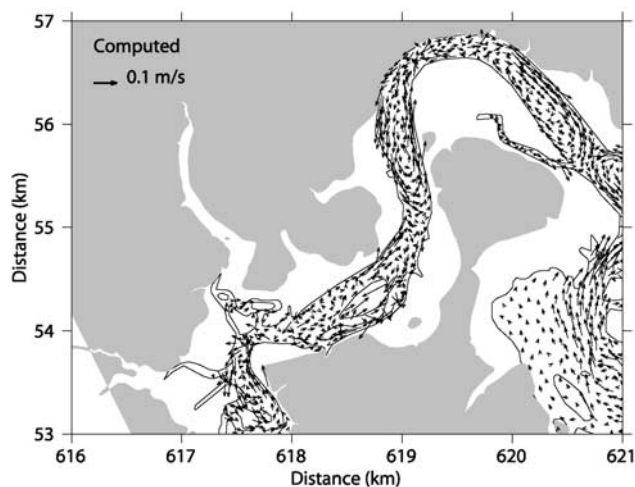


Figure 10. Part of the results from a finite volume numerical model [Chen *et al.*, 2003] that covers the observational area. Shown here is the subtidal flow field.

Table 1. Fraction of Data With $R^2 > 0.7$

Parameter	$M_2 + \text{Mean Only}$	M_2 and $M_4 + \text{Mean}$
Tide	0.75	0.77
Depth-average East Velocity	0.74	0.76
Depth-average North Velocity	0.79	0.81
Near Surface East Velocity	0.60	0.72
Near Surface North Velocity	0.67	0.80

in the Okatee River during the observational period appears to be driven by low-frequency sea level variations [e.g., Wilson *et al.*, 1985]. The actual mechanism of the transport in this system, however, is complicated because of the irregular bathymetry, variable channel width and orientation, and extensive intertidal salt marsh, which contribute to an already highly nonlinear flow field. A more detailed study of this system may require a well-designed numerical modeling experiment. Such a model has been developed based on a finite volume method [Chen *et al.*, 2003] and applied to the Okatee River system. While the detailing of this model requires a separate paper, we demonstrate the subtidal flow calculated from the model, which shows some agreement in spatial distribution with the observations of a downstream flow along the channel (Figure 10). The model results also demonstrate some return (upstream directed) flows in shallow waters that could not be covered by the observations.

5.2. Additional Statistical Assessment

[19] The harmonic-statistical analysis demonstrates some contrast in results obtained with M_4 or without, and results for the tidal elevation and those for velocity. The R^2 value given by equation (10) is a measure of the quality of the fit between the real data and the selected tidal signal. When its value is one, the data contain only the tidal signal at the selected frequencies (i.e., a perfect fit). When its value is zero, the variation of the data is completely nontidal (here “tidal” means tidal components plus a constant).

[20] For a quantitative examination, we group the R^2 values within different ranges of distributions for water depth, depth-averaged velocity components, and near-surface (2 m below the low water level) velocity components. Specifically, we use 10 groups of R^2 values centered at 0.05, 0.15, 0.25, 0.35, 0.45, 0.55, 0.65, 0.75, 0.85, and 0.95, with a uniform range of 0.1. We then calculate the percentage of data that fall into each range of R^2 value and examine their distribution.

[21] When the M_4 constituent is included, we have about 11%, 22%, and 44% of the depth (tide) data with R^2 values within the intervals of (0.7, 0.8), (0.8, 0.9), (0.9, 1.0), respectively. Therefore a total of 77% of the depth data have an R^2 larger than 0.7, a 2% increase from the results without considering the M_4 tide (Table 1).

[22] Similar conclusions hold true for the velocity components. For the depth-averaged tidal velocity vector and excluding the M_4 tidal constituent in the harmonic-statistical analysis, about [11%, 6%], [44%, 31%], and [20%, 41%] (corresponding to [east velocity, north velocity]) of the velocity data have R^2 values within the intervals of (0.7, 0.8), (0.8, 0.9), (0.9, 1.0), respectively. In other words, [74%, 79%] of the velocity vector data have R^2 larger than 0.7 (Table 1).

[23] In contrast, for the depth-averaged tidal velocity including the M_4 tidal constituent in the harmonic-statistical analysis, about [6%, 5%], [30%, 10%], and [40%, 66%] of the velocity vector data have R^2 values within the intervals of (0.7, 0.8), (0.8, 0.9), and (0.9, 1.0), respectively. In other words, [76%, 81%] of the velocity data have R^2 larger than 0.7 (Table 1). The comparison between the depth-averaged velocity and the near-surface velocity are similar, except that the latter has a larger spread and lower percentages of “good fits.” The difference between the results for the near-surface velocity with or without M_4 tidal constituent is up to 12% (the difference between the numbers in right and left columns of the last two rows in Table 1). The results for the velocity at different depths are similar to those of depth-averaged velocity, and the mid-depth data have statistical characteristics closest to that of the depth-averaged velocity. We omit the discussion of velocity at different depths because of its similar nature to the depth-averaged and near-surface velocities due to the vertically well-mixed conditions.

5.3. Improvement of Observations

[24] The data quality can be improved by maintaining a slower vessel speed during the survey. A slower vessel speed, however, will necessarily reduce the length of the survey track for the same number of repetitions. For future studies, depending on the main objective, either a slow vessel speed in combination with a smaller survey area can be adopted for a better data quality, or a faster speed can be chosen for a larger spatial coverage. The data quality can be further improved by reducing ship tracks over areas with large bottom slopes and irregular topography. Although the maximum bottom slope in the present study area is smaller than that of the Chesapeake Bay [Li *et al.*, 2000], it can still reach at least 0.0075 at the channel turns. As shown by Li *et al.* [2000], when the bottom slope is larger than 0.006, the R^2 values could be significantly affected by the bottom slope.

[25] This methodology can be applied in other systems to obtain high-resolution distributions of both tide and velocity data and to validate fine grid numerical models. This is particularly important for complicated tidal creek systems in which flow variability can be large and a limited number of mooring observations may not be enough for the validation of a high-resolution model. Mooring observations sometimes may also be problematic because of boat traffic. Using a small boat to operate surveys such as those presented here can be an efficient and cost-effective way to obtain spatial distributions of tide and tidal flows for different applications, including numerical model validations.

6. Summary

[26] In summary, we have used data from a vessel-towed ADCP to infer tidal constituents for both tidal flow and tidal elevation along the Okatee River, South Carolina. We have used a harmonic-statistical analysis for both the surface elevation and the velocity components. The analysis shows that a higher percentage of the variability in the along-channel velocity can be explained by tidal oscillations; that is, the along-channel velocity is “more tidal” than the cross-channel velocity. When the harmonic analysis includes only

the M_2 and mean component, about 75% of the covered area along the ship track has “good fit” (that is, at least 70% of the variability can be explained by the tidal and mean components). By adding the M_4 component to the harmonic analysis, an additional 2% of the covered area has “good fit” for elevation and depth-averaged velocity. The percentage of “good fit” increases more (up to 12%) for the near-surface and near-bottom velocities which have the largest deviations from the depth-averaged velocity.

[27] Using the method proposed above, we have obtained the tidal and statistical parameters for both surface elevation and velocity along an 8-km longitudinal track in the Okatee River. We have determined that the phase difference between the elevation and velocity is around 90° , and therefore the tidal wave in the Okatee River has the characteristics of a standing wave. This is because of the short length of the channel compared to the quarter wavelength of the tidal wave (~ 70 km for an average depth of ~ 5 m). As a result, the amplitude of surface elevation has no apparent along-channel variation, while the amplitude of the velocity has a significant decrease upstream. Previous studies using vessel-towed ADCPs have been able to resolve the parameters for tidal velocity only. More importantly, previous studies ignored the surface variation due to tides, while in this study the vertical coordinates are corrected according to tidal elevation. We also note that the quality of the results depends highly on variations in the bottom slope and the vessel speed. The standard errors of tidal elevation and velocity from this study appear to be larger than those from ADCP observations across the Chesapeake Bay mouth [e.g., Li *et al.*, 2000]. Nevertheless, we have shown that the method developed in this work can be a useful tool to resolve tide and flow structures as well as to describe their statistical characteristics using a vessel-based ADCP.

[28] **Acknowledgments.** This work is sponsored by the NOAA Coastal Ocean Program through the South Carolina Sea Grant Consortium pursuant to National Oceanic and Atmospheric Administration Award NA960PO113, Georgia Sea Grant Award RR746-007/7512067 and R/HAB-12-PD, and Georgia DNR Award RR100-279-9262764. Constructive review comments from Linda Huzzey and an anonymous reviewer are very much appreciated. S. Elston kindly provided some editorial comments. Participants of the field program included J. Amft, T. Moore, C. Burden, S. Elston, and D. Duarte from the University of Algarve, Portugal. R. Thomas was the captain of R/V *Gannet*, the SKIO's vessel used in this study. The dedication and contribution of these participants to the field work are highly appreciated.

References

- Aubrey, D. G., and P. E. Speer (1985), A study of non-linear tidal propagation in shallow inlet/estuarine systems: I. Observations, *Estuarine Coastal Shelf Sci.*, *21*, 185–205.
- Blanton, J. O., G. Lin, and S. A. Elston (2002), Tidal current asymmetry in shallow estuaries and tidal creeks, *Cont. Shelf Res.*, *22*, 1731–1743.
- Brubaker, J. M., and J. H. Simpson (1999), Flow convergence and stability at a tidal estuarine front: Acoustic Doppler current observations, *J. Geophys. Res.*, *104*, 18,257–18,268.
- Chen, C., H. Liu, and R. C. Beardsley (2003), An unstructured, finite-volume, three-dimensional, primitive equation ocean model: Application to coastal ocean and estuaries, *J. Atmos. Oceanic Technol.*, *20*, 159–186.
- Li, C. (1996), Tidally induced residual circulation in estuaries with cross channel bathymetry, Ph.D. dissertation, Univ. of Conn., Storrs.
- Li, C. (2001), 3D analytic model for testing numerical tidal models, *J. Hydraul. Eng.*, *127*, 709–717.
- Li, C., and A. Valle-Levinson (1999), A two-dimensional analytic tidal model for a narrow estuary of arbitrary lateral depth variation: The intratidal motion, *J. Geophys. Res.*, *104*, 23,525–23,543.

- Li, C., A. Valle-Levinson, L. Atkinson, and T. C. Royer (2000), Inference of tidal elevation in shallow water using a vessel-towed ADCP, *J. Geophys. Res.*, *105*, 26,225–26,236.
- Lwiza, K. M. M., D. G. Bowers, and J. H. Simpson (1991), Residual and tidal flow at a tidal mixing front in the North Sea, *Cont. Shelf Res.*, *11*, 1379–1395.
- Parker, B. (1991), The relative importance of the various non-linear mechanisms in a wide range of tidal interactions (review), in *Tidal Hydrodynamics*, edited by B. Parker, pp. 237-268, John Wiley, New York.
- Proakis, J. G., and D. G. Manolakis (1992), *Digital Signal Processing-Principles, Algorithms, and Applications*, 969 pp., Macmillan, New York.
- Wilson, R. E., K.-C. Wong, and R. Filadelfo (1985), Low-frequency sea level variability in the vicinity of the East River tidal strait, *J. Geophys. Res.*, *90*, 954–960.
-
- J. Blanton and C. Li, Skidaway Institute of Oceanography, 10 Ocean Science Circle, Savannah, GA 31411, USA. (chunyan@skio.peachnet.edu)
C. Chen, School of Marine Science and Technology, University of Massachusetts-Dartmouth, New Bedford, MA, USA.